

Increased abundance of MTD1 and MTD2 mRNAs in nodules of decapitated *Medicago truncatula*

Paola M.G. Curioni¹, Beat Reidy¹, Thomas Flura¹, Regina Vögeli-Lange², Josef Nösberger¹ and Ueli A. Hartwig^{1,*}

¹Institute of Plant Sciences, Swiss Federal Institute of Technology, Universitätstrasse 2, 8092 Zürich, Switzerland (*author for correspondence; e-mail: ueli.hartwig@ipw.agr.ethz.ch); ²Botanisches Institut der Universität Basel, Hebelstrasse 1, 4056 Basel, Switzerland (current address: Novartis AG, Postfach, 4002 Basel, Switzerland)

Received 27 August 1999; accepted in revised form 20 June 2000

Key words: decapitation, mRNA differential display, nitrogenase activity, nodule

Abstract

To gain insight into the molecular processes occurring in root nodule metabolism after stress, we used a mRNA differential display (DDRT-PCR) approach to identify cDNAs corresponding to genes whose expression is enhanced in nodules of decapitated *Medicago truncatula* plants. Two full-length cDNAs of plant origin were isolated (MTD1 and MTD2). Sequence analysis revealed that MTD1 is identical to an EST clone (accession number AW559774) expressed in roots of *M. truncatula* upon infection with *Phytophthora medicaginis*, while MTD2 is highly homologous to an *Arabidopsis thaliana* gene (accession number AL133292) coding for a RNA binding-like protein. The two mRNAs started to accumulate in root nodules at 4 h after plant decapitation and reached even higher transcript levels at 24 h from the imposition of the treatment. MTD1 and MTD2 mRNAs were mainly induced in nodules, with very little induction in roots. The abundance of the two transcripts did not change in response to other perturbations known to decrease nitrogenase activity, such as nitrate and Ar/O₂ treatments. Our results suggest that MTD1 and MTD2 represent transcripts that accumulate locally in nodules and may be involved in changes in nodule metabolism in response to decapitation.

Introduction

In legume root nodules, the bacterial enzyme nitrogenase catalyses the reduction of dinitrogen gas to ammonia. Nitrogenase activity is rapidly inhibited by a series of treatments that affect plant C and N metabolism, such as stem girdling, defoliation, decapitation (shoot removal, defoliation), nitrate fertilization, drought and replacement of the N₂ in the rhizosphere with Ar (Hartwig, 1998). Forage legumes in many temperate regions of the world are subjected to various degrees of defoliation either by grazing animals or by mechanical harvest. Harvesting the shoots of legumes causes instantaneous reduction of both

C translocation to the roots and mineral N uptake. Further, leaf removal drastically decreases nodule N₂ fixation within a few hours (Ryle *et al.*, 1985; Hartwig *et al.*, 1987, 1990, 1994; Gordon *et al.*, 1990; Denison *et al.*, 1992; Heim *et al.*, 1993). However, the interruption of the supply of photosynthate to the nodules after decapitation does not seem to be the immediate cause of the decline in nitrogenase activity (Hartwig *et al.*, 1990, 1994; Denison *et al.*, 1992; Weisbach *et al.*, 1996; Curioni *et al.*, 1999). In most cases, this decline can be overcome by increasing the O₂ concentration in the rhizosphere. Thus, the decrease in nitrogenase activity has been attributed to a decrease in nodule O₂ permeability, which is thought to be regulated by a variable oxygen diffusion barrier in the nodule inner cortex (Sheehy *et al.*, 1983; Witty *et al.*, 1984, 1986). However, the exact nature and mech-

The nucleotide sequence data reported will appear in the EMBL, GenBank and DDBJ Nucleotide Sequence Databases under the accession numbers AF180292 (MTD1) and AF180293 (MTD2).

anism of regulation of such a barrier is still poorly understood and, therefore, the primary effect responsible for the decline in nitrogenase activity after stress is still obscure.

One may expect that the response of root nodules to a drastic environmental perturbation, such as decapitation, is characterized by a series of physiological and biochemical changes that ultimately result in the selective increase or decrease in the biosynthesis and/or degradation of distinct proteins. The resulting differences in protein patterns are due, at least in part, to changes in the transcription of the corresponding genes. In the past, much attention has been given to the mobilization of N reserves during regrowth of defoliated white clover (Corre *et al.*, 1996) and alfalfa (Avice *et al.*, 1997). These studies examined the changes in soluble proteins, such as vegetative storage proteins (VSPs), in the roots of the plant on a long-term basis. In nodules, it was found that defoliation of white clover causes the loss of certain proteins, including leghemoglobin, as assessed by PAGE and autoradiography after *in vivo* assimilation of ^{35}S -methionine by nodules (Gordon *et al.*, 1990) and western immunoblotting (Gordon and Kessler, 1990). However, changes in gene expression may be occurring hours or days before major changes in enzyme or protein levels become evident. Therefore, we decided to use a mRNA differential display approach to investigate changes in gene expression in *M. truncatula* root nodules immediately after decapitation in order to get insight into related, underlying processes involved in the regulation of nitrogenase activity. Therefore, we also investigated a possible correlation of the changes in gene expression with reduced nitrogenase activity as a result of decapitation, nitrate and Ar/O₂ treatments.

Materials and methods

Plant growth conditions

Seeds of *Medicago truncatula*, genotype A17, were surface-sterilized in 70% v/v ethanol for 3 min, rinsed with double-distilled water, allowed to germinate on 1.5% water agar and then planted in 2-litre pots filled with silica sand (0.8–1.2 mm grain size). Plants used for gas-exchange measurements and Ar/O₂ treatment (see below) were grown in 250 ml gas-tight sealable pots. Plants were grown in growth chambers (PGR-15, Conviron Instruments, Winnipeg, Manitoba, Canada)

at 20/16 °C day/night temperature and 80% relative humidity, with a 16 h photoperiod and a photon flux density of 500 $\mu\text{mol PAR m}^{-2} \text{s}^{-1}$ (fluorescent (Cool White, 160 W) and incandescent (138 L 100 W), Sylvania GTE, Geneva, Switzerland). Plants were watered with nitrogen-free nutrient solution (Hammer *et al.*, 1978) and inoculated with *Sinorhizobium meliloti* strain 1021. All experiments were performed when plants were 8–9 weeks old.

Nitrogenase activity measurements after decapitation

Nitrogenase (EC 1.18.6.1) activity was measured *in situ* as H₂ evolution in an open flow gas-exchange system similar to that described by Minchin *et al.* (1983) and modified by Heim *et al.* (1993). The nodulated root systems of the plants were sealed into their pots and allowed to stabilize overnight for 18–20 h in a gas stream of ambient air at 250 ml/min. Prior to the imposition of the decapitation treatment, the flow rate was increased to 400 ml/min and the root systems were exposed to a gas stream of N₂/O₂ (80:20, v/v) for at least 1 h until steady-state rates of H₂ evolution were established. Total nitrogenase activity (TNA) was determined as peak H₂ evolution in Ar/O₂ (80:20, v/v).

Decapitation, argon and nitrate treatments

The decapitation treatment involved the removal of all of the above-ground parts of the plants.

The control plants were intact plants, harvested at the same time points as the decapitated plants, i.e. 2 h, 4 h, 24 h after decapitation. For the Ar treatment, plant root systems were continuously exposed to a gas-flow of Ar/O₂ (80:20, v/v) as described before. The control plants were plants whose root systems were exposed to N₂/O₂ (80:20, v/v). Both Ar-treated and control plants were harvested after 4 h of treatment. For the nitrate treatment, plants were watered with 15 mM nitrate solution for 2 days while control plants were watered with N-free nutrient solution. In all the experiments, plants were quickly uprooted and then the nodulated root systems were rinsed in distilled water, blotted dry and immersed in liquid N₂. Nodules were picked while still frozen. Leaf material was immediately frozen in liquid N₂ and all the plant material was then stored at –80 °C. Before extracting RNA, nodule samples were prepared in a bath of liquid N₂ by carefully removing any root fragments and sand under a magnifying glass. Root samples were prepared by removing nodules and sand particles according to the same procedure.

Nucleic acid isolation

For the differential display, total RNA was extracted by a hot phenol method as described by Mohr *et al.* (1998). For subsequent northern gel blot analyses, total RNA was extracted as described by Chirgwin *et al.* (1979). Genomic DNA from *M. truncatula* leaves was extracted using the DNeasy plant mini kit (Qiagen, Chatsworth, USA) or the Plant DNA Isolation Kit (Roche Molecular Biochemicals, Rotkreuz, Switzerland). Genomic DNA from *S. meliloti* suspension cultures was extracted using the DNeasy Tissue Kit (Qiagen) according to the manufacturer's instructions.

Differential display of mRNA (DDRT-PCR)

Total RNA from nodules of control and 4 h decapitated plants was isolated as described above. The RNA samples were treated with DNase I using the MessageClean Kit according to the manufacturer's recommendations (GeneHunter, Brookline, USA). Further manipulations followed the protocol of Liang *et al.* (1993) and Liang and Pardee (1992) and were carried out essentially according to the RNAimage manual (GeneHunter). Briefly, reverse transcription (RT) reactions were performed using one-base anchored oligo-dT primers (Liang *et al.*, 1994) and 0.2 μ g DNase I-treated RNA. The resulting cDNA preparations were used as template in PCR amplifications with the same oligo-dTs as used for the reverse transcription in combination with arbitrary 13-mer primers (GeneHunter) in the presence of [α -³³P]dATP and in a 20 μ l total reaction volume. The thermocycler (Genius, Techno, Princeton, NJ) conditions were as follows: 94 °C for 30 s, 40 °C for 2 min and 72 °C for 1 min, for 30 cycles, and a final elongation step at 72 °C for 5 min. PCR products were separated on a 7 M urea/6% sequencing gel (Sambrook *et al.*, 1989). To estimate the size of cDNA bands, a *PhiX* 174/*Hinf*I DNA marker (Stratagene, La Jolla, CA), end-labelled with [α -³³P]dATP using a Klenow Fill-in Kit (Stratagene), was loaded on the gel. Then gels were dried and exposed to X-ray film (Biomax, Kodak) for 24 h. Bands of interest were excised and the DNA was eluted from the gel fragments essentially as described by Johnson *et al.* (1995). DNA preparations were then reamplified with the same primer sets and PCR conditions as for the original DDRT-PCR reactions. Re-amplified cDNAs were analysed on a gel and cloned into the pGEM-T vector (Promega, Madison, WI). Blue/white selected colonies were screened for plasmids with inserts by PCR, using the appropriate primer combinations. For

each differential display band, ten colonies containing the inserts of correct size were chosen for further analysis. To differentiate between colonies containing cDNAs from truly differentially expressed genes and those generated from contaminating constitutively expressed genes, a reverse northern blot analysis was performed as described by Vögeli-Lange *et al.* (1996, 1997). Briefly, cloned cDNA fragments were amplified by colony PCR. The products were loaded in duplicate sets onto NY13 N nylon membranes (Schleicher and Schuell, Dassel, Germany) with a slot blot apparatus (BRL, Gaithersburg, MD). One membrane was hybridized with the original [³³P]-PCR product from the control sample used in the DDRT-PCR, while the other membrane was hybridized with the [³³P]-PCR product from the treated sample. After high-stringency washes, hybridization signals were visualized using a GS-250 Molecular Imager (BioRad, Hercules, CA) and the corresponding bands compared.

Sequence analysis

Cloned cDNAs were sequenced automatically by using a laser-induced fluorescence capillary system (ABI Prism 310 Genetic Analyzer, Perking Elmer, Norwalk, CT). Sequence analysis was carried out with GCG software (Genetics Computer Group, Madison, WI) and the BLAST network services at the National Centre for Biotechnology Information.

Cloning of full-length cDNAs

Full-length cDNAs were obtained with the SMART RACE cDNA Amplification Kit (Clontech, Palo Alto, CA). Total RNA (10 μ g), extracted from nodules harvested at 4 h after plant decapitation, was transcribed into cDNA with SuperScript II reverse transcriptase (Life Technologies, Rockville, MD), according to the manufacturer's instructions. Products were used for 5'-PCR amplification with an anchor-specific primer mix and one gene-specific primer (MTD1: CACTATGATGGATGATGAGTTGTTTC; MTD2: GAAAGGGCAATATAACAACCCTTACC). Obtained products were subjected to a nested PCR reaction using a nested anchor primer and nested gene-specific primers (MTD1: GTTGCAGCAATGGCACAATGATGC; MTD2: TGTCCTAACATCAACAATGTCAC). The resulting DNA fragments were sub-cloned into pGEM-T easy vector (Promega) and analysed by sequencing (Microsynth, Balgach, Switzerland).

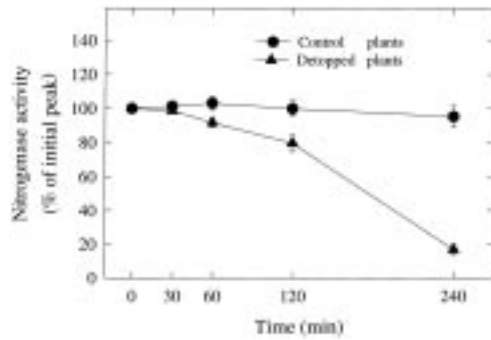


Figure 1. Effect of decapitation on total nitrogenase activity (TNA) in *M. truncatula* nodules. TNA was determined as peak H_2 evolution rate in Ar/O_2 (80:20, v/v). Data are expressed as a percentage of initial TNA before decapitation. Each data point represents the mean \pm SE of 5 replicate plants. The average apparent nitrogenase activity (ANA, H_2 evolution rate in N_2/O_2 , 80:20, v/v) before decapitation was $1.3 \pm 0.2 \mu\text{mol}$ per gram root dry weight per hour.

Northern blot analysis

All manipulations were carried out according to standard procedures (Sambrook *et al.*, 1989). Total RNA (10 μg per lane) was electrophoresed in 1.1% agarose gels containing 0.65 M formaldehyde. RNA was transferred onto a NY13 N nylon membrane (Schleicher and Schuell) by capillary transfer in the presence of $20\times$ SSC and subsequently UV cross-linked. To verify equal loading and transfer of RNA, filters were stained with methylene blue, according to Herrin and Schmidt (1988). Probes were generated by colony PCR and purified with the GeneClean II Kit (BIO101, Vista, CA) after gel electrophoresis. Then, 25 ng purified PCR product was labelled with $[\alpha\text{-}^{32}\text{P}]\text{dATP}$ with the Prime-It II Random Primer Labeling Kit (Stratagene) following the manufacturer's instructions. Membranes were hybridized overnight and the final wash was carried out at 60°C in $0.2\times$ SSC, 0.5% SDS. Blots were exposed to X-ray films for 1 to 2 days.

Southern blot analysis

Genomic DNA (7.5 μg) was digested with *Pst*I, *Eco*RI or *Hind*III, separated on a 0.8% agarose gel and transferred onto Nytran membranes (Schleicher and Schuell). Blotting and hybridization were performed under standard conditions (Sambrook *et al.*, 1989). The blot was hybridized at 65°C with the randomly ^{32}P -labelled full-length MTD1 and MTD2 probes. Membranes were washed to a final stringency of $0.2\times$ SSC, 0.5% SDS at 50°C before autoradiography at -80°C using intensifying screens.

Results and discussion

Effect of decapitation on total nitrogenase activity

Total nitrogenase activity was assayed as H_2 evolution in Ar/O_2 (Figure 1). The nodulated root systems of both control and decapitated plants were exposed to N_2/O_2 for the duration of the experiment except for brief periods when the gas mixture was switched to Ar/O_2 to assay total nitrogenase activity. Decapitation caused a slow steady decline to about 80% of the initial activity in the first 2 h after decapitation. Subsequently, a more dramatic decline was observed and at 4 h after decapitation, the activity was less than 20% of the initial one (Figure 1). The decline in total nitrogenase activity seems to occur later in decapitated *M. truncatula* plants than in other species. In decapitated *Medicago sativa* (Curoni *et al.*, 1999) and in completely defoliated *Trifolium repens* (Hartwig *et al.*, 1994), nitrogenase activity declined to about 20% of the initial value within 2 h.

Identification of decapitation-enhanced mRNAs by differential display of mRNA

In order to identify decapitation-enhanced plant genes, we used the mRNA differential display (DDRT-PCR) method as described in Materials and methods. *M. truncatula* plants were decapitated and nodules were harvested at 4 h after decapitation. Control nodules were from non-decapitated plants. RT-PCR was performed on extracted RNA with several primer combinations and PCR products were analysed on a sequencing gel. Each primer combination resulted in a characteristic highly reproducible banding pattern (data not shown). Several bands of both stronger and weaker intensities were identified in the samples from nodules of decapitated plants but they have not been completely characterized. Three bands (MTD1, MTD2 and MTD3) that showed higher intensity upon decapitation (Figure 2a) were excised. The eluted DNA was re-amplified by PCR and the resulting cDNAs used for cloning.

One of the major problems of the differential display technique is the generation of a relatively large number of false-positives. This arises from the fact that a single DDRT-PCR band is often composed of several bands, many of which derive from constitutively expressed genes. To circumvent this problem, several positive clones from a single differential display gel band were examined by reverse northern blot analysis. Figure 2b shows an example of reverse

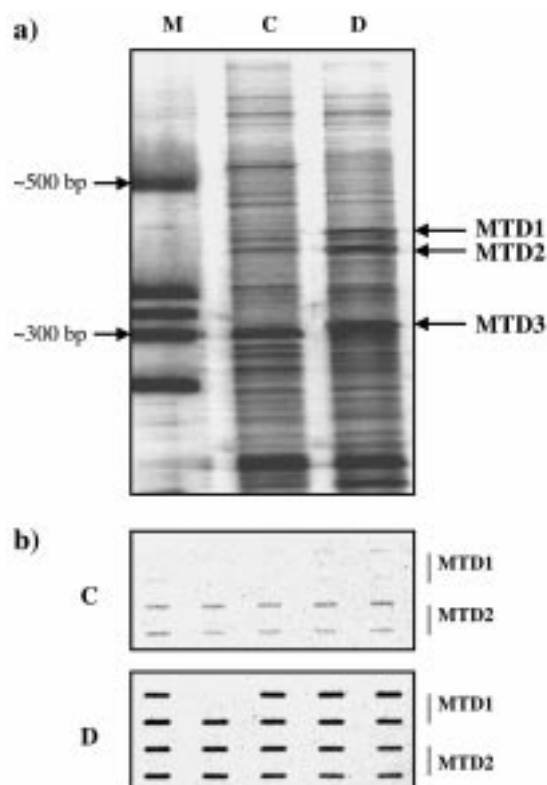


Figure 2. Region of differential display gel showing decapitation-enhanced mRNAs. RNA showing decapitation-enhanced mRNAs. RNA samples were from nodules of control *M. truncatula* plants (C) and from nodules of decapitated plants (D) harvested at 4 h after the imposition of the treatment. Differentially expressed cDNAs which were subsequently cloned are indicated by arrows. The approximate size of the DNA fragments of the molecular weight marker (M) are indicated on the left side of the figure. b. Selection of clones with cDNA inserts from differentially expressed genes by reverse northern blot analysis, utilizing DDRT-PCR products as hybridization probes. PCR amplified inserts of sets of 10 individual *E. coli* colonies, obtained by transformation with MTD1 and MTD2, were immobilized onto nylon membranes in duplicate sets and hybridized with the original ^{33}P -PCR product from nodules of control plants (C) or from nodules of decapitated plants (D).

northern blot analysis for the identification of cDNA fragments derived from truly differentially expressed genes. By comparing the hybridization patterns, all the clones but one appeared to contain a cDNA insert of a gene whose expression is up-regulated in nodules of decapitated *M. truncatula* plants.

To further verify the expression pattern of the differentially displayed bands, northern blot analyses were performed. cDNA clones corresponding to the decapitation-enhanced transcripts MTD1 and MTD2 were used to probe blots containing total RNA from nodules of control and 4 h decapitated plants. The re-

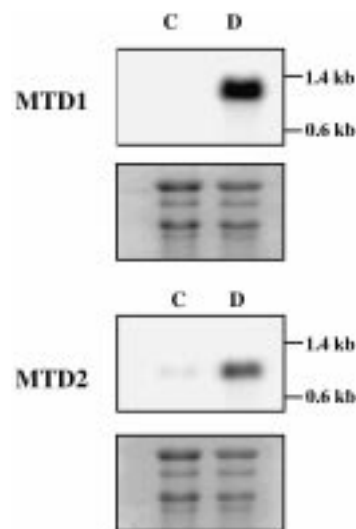


Figure 3. Expression pattern of decapitation-enhanced mRNAs. Total RNA ($10\ \mu\text{g}/\text{lane}$) from the same samples (C, D) used for the differential display analysis (Figure 2a) was fractionated by denaturing agarose gel electrophoresis, blotted onto nylon membranes and hybridized with the radiolabelled MTD1 (panel a) and MTD2 (panel b) cDNA probes. The approximate size of the hybridizing mRNAs was estimated by comparison to RNA size markers (Promega). As a loading control, rRNA bands of methylene blue-stained membranes are shown in the respective lower panels.

sults (Figure 3) provide further proof that the cDNAs identified represent mRNAs that accumulate in nodules at 4 h after decapitation.

Sequence analysis of decapitation-enhanced mRNAs

The full-length cDNA sequences of MTD1 (Figure 4a) and MTD2 (Figure 4b) were determined. MTD3 was not further considered since its sequence was found to be identical to a portion of the MTD1 sequence (data not shown). This can arise from the fact that a particular sequence can be over-represented due to the use of different polyadenylation sites which results in different lengths and different anchors for the reverse transcription (Joshi, 1987). The full-length cDNA sequences for MTD1 and MTD2 were found to be 945 bp and 853 bp, respectively.

Database searches (Altschul *et al.*, 1997) revealed that MTD1 corresponds to an EST clone (accession number AL133292) expressed in roots of *M. truncatula* upon infection with *Phytophthora medicaginis*. MTD2 shares 58% amino acid identity and 75% amino acid similarity (over a length of 232 amino acids) with a RNA binding-like protein located on chromosome 3 of *Arabidopsis thaliana* (accession number CAB61962).

a) MTD 1		b) MTD2	
GGTGCTATCTCTCTTTTCCCTTCATCTCTTTGGTGTGTTGTTGATTATGGAG	51	GGGCACACAAAAATTCAGTGAAAATCTTTTGGTATGGGAAAGAGTTTG	51
			M G K S L
CTTGAACCGGTGCCGTTTAAOCCGGTGGGATCACGTACTCCGTTGTTAITT	102	TTTCAAGAATCTCTGAAAGCTCTAGAAGCTGATATTCAGTATGCTAATACA	102
L E T V A F K R V G S R T S V L F		F Q E S L K A L E A D I Q Y A N T	
GACCGCCAAAGGATCATGATGATGATCAAGGGAAGGTGTAGTACGACG	153	CTGCCATTAGTTCATCCAAGGGATAAAGAAGGAGGATGCTTTCAAATGAGG	153
D A P R D H D D D Q G K V C S T T		L A L G H P R D K E G G C F Q M R	
TCGTCTTCATCGATCGAAGAAATAGTGATGATGATGATGATGATGAGGTT	204	CTATCATACAGTCCAGTGGCCCGACTTTTCTCTCTCTTGTTCAGTGGACT	204
S S S S I G R N S D D D D D D E V		L S Y S P V A P L F L S L V Q W T	
TCATCGGAAAGATCAATGGATGAGAATGAAGCTGAGAGTAAATATAATGGT	255	GATACCGACTTGTGGTGGTCTTGGTGGTCTCAGAAATCTAATTTATGTG	255
S S E R S M D E N E A E S K Y N G		D Y R L A G A L G L L R I L I Y V	
GGTGCCTTAGATTGATGGAAAGCTTTAGAAGAGGTTCTCTCTATTAGGAGA	306	ACATATGGAAATGGGAGACTACTATTTCAATTTATGAAAGGAAAGCAAGC	306
G A L D C M E A L E E V L P I R R		T Y G N G K T T I S I Y E R K A S	
AGTATCTCAAATTTCTACAGTGGGAAGTCTAAGTCTTCAACAAGCTAGCT	357	ATAAGACAATTTTATTCGATTATATTTCTCTCTCTATTCGAACTTCAGAAA	357
S I S N F Y S G K S K S F T S L A		I R Q F Y S I I F P A L L Q L Q K	
GATGTTGTGACCAACCCATCTGTAAAAGACATTTGAAAACAGAGATGCA	408	GGTGTACAGATTTGGAAGAAAGGAGCAGAAAGATATATGCTAATAGA	408
D V V T T P S V K D I V K P E N A		G V T D L E E R K Q K E V Y A N R	
TACACAAGAACGATGAGAATTTGCTGGCTTTCAATCATGGTTGGGACAAG	459	TATCAAAAGAGACTGATTTCAAAGATAGAAGAGATCTAAAATTGACATT	459
Y T R R R R N L L A F N H G W D K		Y Q K K T D F K D R R E S K I D I	
AACAAAAATTTCCCTTTGAGAAGCAATAGTGGTGGCAATTTCAAAGAGAAC	510	GAAAGAGAAAAAGAAATGCGGAGTTTGCCTGGAGGTGAAAGCAAAAGTTGG	510
N K N F P L R S N S G G I S K R T		E R E K E C G V C L E V K A K V V	
ATGAGCTTAAAGTGAAGTGCCTTTCCTCTGTCAGTTCATTAAGCAATTTCT	561	CTGCCTAATTTGGCCACCAATGTGTTTCAAGTGTTCACAGAGAATGGTGT	561
M S L S R S A L A L A V A L S N S		L P N C C H Q M C F K C Y R E W C	
GATAGCAGCTTCTAGTTTACAAGTGTGATTCAGTCTACTTCAACCTCATAT	612	CITTAGGTCTCAATCTTCCCGCTTTTCCCGGATAGCTTGAAGAGAGTGAAC	612
D S S S S P T S D D S A T S T S Y		L R S Q S C P F C R D S L K R V N	
TCTTCAGCAGCTTCAATCACCAGTTCGCCCGGTGATCCGGGAAATAGAGTG	663	TCTGGTGAAGTTGGATTTACACAGACACAAGTACATTTGTTGATTTGGG	663
S S A P S S P L P P R H P G N R V		S G D L W I Y T D T S D I V D V G	
TCTTCTTTCAGCATCTCTTTCAGAGAAATTTCTTTCCTTGGCTGATTGG	714	ACAAATTTCAAAGAGAATTTGAAGATTTCTGTTCTTTCATAGAAAAGTTG	714
S S L A S P L Q R N F F S L A D L		T I F K E N C K I L F L Y I E K L	
CATCATTGTGCGATTGCTGCAACAATGAAATGCCAAGTTCCTCAATGAA	765	CCACTTATATTCCAGACCCCAAGCATGGTGCATATGATCCATTTTITAGG	765
H H C A I A A T M K M P S S S I E		P L I I P D P R H V S Y D P F F R	
AATGAAACAACATCATCATCATCATGATGATGATAAAACCTTATGATAACTAA	816	TAAGGGTGTATATTTGCCCTTTCATGACTTGTAAATCCATTTTGGACAA	816
N E T T H H P S *		*	
AATACAACGTTTATTAACCTTTTATAATCTCATTTGGATGAGTTTCTTG	867	TAATTTAATTTGAAATATTCTAGTGTAAAAAATAA	853
CTCTAGTCTATTTTGTGTGAGCGAGAAAGAGGTTATAGAATAAAATCATA	918		
GATAAATCTTTTTAGTAAAAAATAA	945		

Figure 4. Nucleotide sequences and deduced amino acid sequences of MTD1 (a) and MTD2 (b). Underlined nucleotides show gene-specific primers used for the 5'-RACE. Stop codons are indicated by an asterisk (*). Nucleotides in bold face correspond to the arbitrary primers used for the differential display reaction.

Genomic origin of decapitation-enhanced mRNAs

M. truncatula root nodules are complex symbiotic structures in which mRNAs of both plant and bacterial origin are present. We decided to determine the genomic origin of the decapitation-enhanced mRNAs by PCR analysis. Genomic DNA from *M. truncatula* leaves and *Sinorhizobium meliloti* liquid cultures was extracted and used as template in PCR reactions, performed with MTD1 and MTD2 sequence-specific primers or for Southern blot analysis. The results are summarized in Figure 5. An amplification product was observed only when genomic DNA from *M. truncatula* leaves was used as template in the PCR reaction, while no amplification product was detected when genomic DNA from *S. meliloti* liquid cultures was used as template (Figure 5a). Further, as the amplification product for MTD2 is larger (about 1.2 kb) than expected (about 0.3 kb), we hypothesize the presence of one or more introns. To avoid artefacts and

to show that the PCR reactions were dependent on the presence of both sequence-specific primers, PCR reactions with a single primer were also performed (Figure 5a). As a positive control for the presence of *S. meliloti* genomic DNA, we used PCR primers that specifically amplify the *S. meliloti* 1021 nirK (nitrite reductase) genes (Braker *et al.*, 1998) (Figure 5b). Southern blot analysis confirmed the plant origin of MTD1 and MTD2 (Figure 5c) as it was successful with genomic DNA from *M. truncatula* leaves while no restriction bands are present in lanes containing digested *S. meliloti* genomic DNA. In addition, for both cDNAs, only one or two major restriction bands are visible in lanes containing digested *M. truncatula* genomic DNA. This suggests that MTD1 and MTD2 are presumably encoded by single or low-copy-number genes.

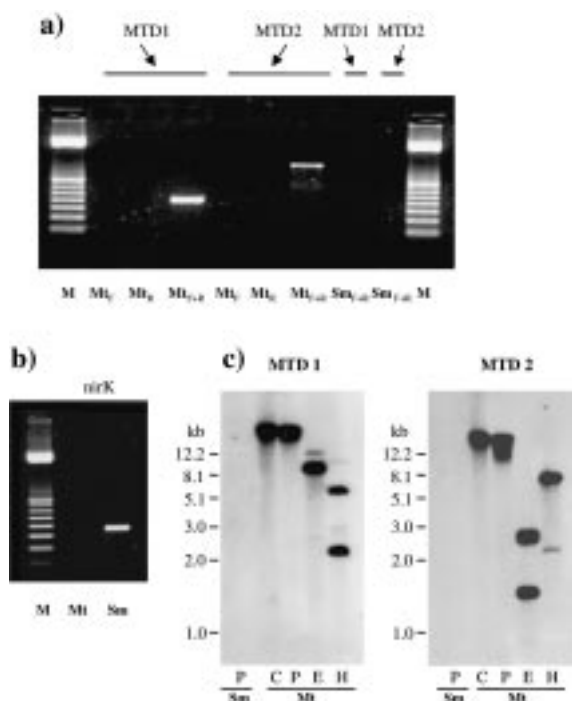


Figure 5. Confirmation of the plant genomic origin of MTD1 and MTD2 by PCR. a. Genomic DNA from *M. truncatula* leaves (Mt) and *S. meliloti* suspension cultures (Sm) was used as template in PCR reactions with MTD1 and MTD2 sequence-specific primers. M indicates a 100 bp ladder. To verify the specificity of the MTD1 and MTD2 primers, PCR reactions with only the forward (F) or reverse (R) primer were performed. b. As a positive control for the presence of *S. meliloti* genomic DNA, a primer pair that specifically amplifies the *nirK* genes of *S. meliloti* 1021 was used (Braker *et al.*, 1998). c. Northern blot analysis of MTD1 and MTD2. Genomic DNA (7.5 μ g) from *M. truncatula* leaves (Mt) and *S. meliloti* suspension culture (Sm) was digested with either *Pst*I (P), *Eco*RI (E) or *Hind*III (H), separated by gel electrophoresis and hybridized with 32 P-radiolabelled MTD1 and MTD2 probes. Lane C shows the undigested DNA control. Final washes were at $0.2\times$ SSC, 0.5% SDS at 50 $^{\circ}$ C. DNA size standards (kb) are given on the left of each blot.

Temporal appearance of MTD1 and MTD2 in *M. truncatula* nodules and roots after decapitation

Northern blot analyses were performed to investigate the expression patterns and the tissue specificity of MTD1 and MTD2 in *M. truncatula*, separately in nodules and in roots, after plant decapitation. Samples were harvested at 2 h, 4 h and 24 h after decapitation. The abundance of the transcripts was monitored using 32 P-labelled MTD1 and MTD2 probes (Figure 6a and b). The MTD1 mRNA is highly induced in nodules at 4 h after decapitation and reaches even higher transcript levels at 24 h after decapitation. A low induction can also be seen in roots starting from 2 h after de-



Figure 6. Effect of decapitation on the expression pattern of MTD1 (panel a) and MTD2 (panel b) in nodules and roots of *M. truncatula* plants, obtained by northern blot analysis. Total RNA (10 μ g/lane) from nodules and roots of non-decapitated (C) and decapitated plants (D) at 2 h, 4 h and 24 h after decapitation was subjected to northern hybridization analysis with radiolabelled MTD1 and MTD2 probes as described in Figure 3. As a loading control, rRNA bands of methylene blue-stained membranes are shown in the respective lower panels. Approximate mRNA sizes are indicated.

capitation. At all time points, the level of MTD1 in control nodules and control roots is close to or below the detection limit of the northern blots (Figure 6a). For the MTD2 mRNA (Figure 6b), we found similar kinetics of transcript accumulation as for MTD1. The MTD2 mRNA is enhanced in nodules of 4 h after decapitation, while the expression level in nodules of control plants remains below the detection limit. The MTD2 transcript seems to be present also in roots of control plants at all time points, albeit its level is weakly enhanced by decapitation (Figure 6b). In general, the expression level of MTD2 is lower than that of MTD1 (Figure 6a and b). These results suggest that MTD1 and MTD2 mRNAs are mainly induced in nodules and the corresponding genes are most likely related to changes in nodule metabolism in response to decapitation.

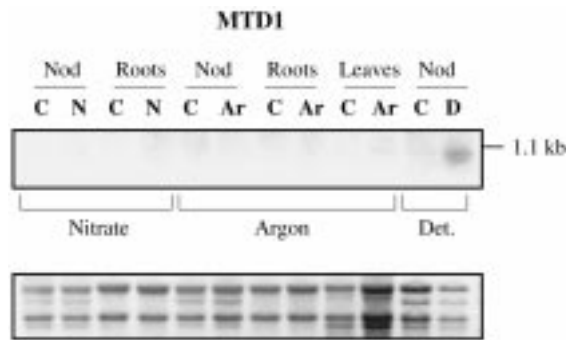


Figure 7. Effect of different treatments on the expression of MTD1. Northern blot analysis of total RNA from nodules (Nod) and roots of control (C) and plants treated with nitrate for 2 days (N); nodules, roots and leaves of control (C) and 4 h Ar/O₂-treated plants (Ar) and nodules of control (C) and 4 h decapitated plants (D). Northern blot analysis was performed as described in Figure 3.

Effect of different treatments on the expression of MTD1 and MTD2

In order to determine whether the accumulation of the MTD1 and MTD2 mRNAs was also triggered by other treatments which result in a decline in nitrogenase activity, we investigated the expression of MTD1 and MTD2 after nitrate and Ar/O₂ treatments. Nitrogenase activity in plants treated for 2 days with nitrate was about 30% of the initial activity measured before the nitrate fertilization. In plants treated with Ar/O₂ for 4 h, nitrogenase activity was about 66% of the peak H₂ evolution rate (data not shown). We isolated RNA from nodules and roots of plants treated for 2 days with nitrate, and from nodules, roots and leaves of plants treated with Ar/O₂ for 4 h. Results for MTD1 are shown in Figure 7. A hybridization signal was observed only in the case of nodules from decapitated plants. No signal was detected in the case of nitrate- and Ar-treated samples. The same was found for MTD2 (data not shown). This suggests that the enhancement of MTD1 and MTD2 is decapitation-specific. However, different mechanisms may operate to reduce nitrogenase activity after these treatments. Thus, we cannot exclude that the accumulation in nodules of the two transcripts, in parallel to the decrease in nitrogenase activity, may be linked to one of these different mechanisms. It seems unlikely that the induction of MTD1 and MTD2 is related to changes in nodule O₂ permeability because it occurs only after decapitation and not after nitrate and Ar/O₂ treatments, which are also known to be associated with a reduction in the nodule permeability to O₂ (see Introduction).

In general, considering that the induction of the two transcripts (Figure 6a) parallels the decrease in nitrogenase activity after decapitation (Figure 1), it is possible that their accumulation is linked to early metabolic processes related to decreased nitrogenase activity after decapitation. Taken together, these results suggest that MTD1 and MTD2 could belong to one of the following classes of genes: (1) genes related to molecular events linked to decreased nitrogenase activity, hence N₂ fixation; (2) genes involved in general stress-related responses, like the ones encoding pathogenesis-related (PR) proteins or those related to wound responses (Lamb *et al.*, 1989; Bowles, 1990; Baron and Zambryski, 1995). The fact that MTD1 corresponds to an EST clone found upon infection with a pathogenic fungus is not surprising as it is known that many of the pathogen-inducible defence responses can also be triggered by mechanical and chemical stresses (Bowles, 1990). It is possible that, in our case, decapitation could have activated responses similar to pathogenic infection in a systemic fashion. However, to further test this hypothesis it would be interesting to carry out a wounding experiment.

At present, though, we cannot give definite explanations. Further experiments would be necessary to investigate the biochemical activities and the localization of the proteins encoded by the genes corresponding to MTD1 and MTD2 and the physiological role they might play. Knowledge about the protein identities would allow us to gain a better understanding of the molecular processes involved in nodule metabolism and how these processes are affected by environmental stress.

Acknowledgements

We wish to thank Dr A. Schaller for generous help with the northern blot analyses. We are extremely grateful to Katinka Beyer, Athos Bonanomi, and H el ene Corbi ere for their help and assistance regarding the differential display technique. We appreciate the co-operation and excellent technical assistance of Werner Wild. We wish to thank Dr C. Sautter for his useful comments on an early draft of the manuscript. We are extremely grateful to Professor N. Amrhein for critically reading the manuscript. This work was supported by a grant from the Swiss Federal Institute of Technology.

References

- Altschul, S.F., Madden, T.L., Sc affer, A.A., Zhang, J., Zhang, Z., Miller, W. and Lipman, D.J. 1997. Gapped BLAST and PSI-BLAST: a new generation of protein database search programs. *Nucl. Acids Res.* 25: 3389–3402.
- Avice, J.C., Ourry, A., Lemaire, G., Volenec, J.J. and Boucaud, J. 1997. Root protein and vegetative storage protein are key organic nutrients for alfalfa regrowth. *Crop Sci.* 37: 1187–1193.
- Baron, C. and Zambryski, P.C. 1995. The plant response in pathogenesis, symbiosis and wounding: variations on a common theme. *Annu. Rev. Genet.* 29: 107–129.
- Bowles, D.J. 1990. Defence-related proteins in higher plants. *Annu. Rev. Biochem.* 59: 873–907.
- Braker, G., Fesefeldt, A. and Witzel, K.P. 1998. Development of PCR primer systems for amplification of nitrite reductase genes (*nirK* and *nirS*) to detect denitrifying bacteria in environmental samples. *Appl. Environ. Microbiol.* 64: 3769–3775.
- Chirgwin, J.M., Przybyla, A.E., MacDonald, R.J. and Rutter, W.J. 1979. Isolation of biologically active ribonucleic acid from sources enriched in ribonuclease. *Biochemistry* 18: 5294–5299.
- Corre, N., Bouchart, V., Ourry, A. and Boucaud, J. 1996. Mobilization of nitrogen reserves during regrowth of defoliated *Trifolium repens* L. and identification of potential vegetative storage proteins. *J. Exp. Bot.* 47: 1111–1118.
- Curioni, P.M.G., Hartwig, U.A., N osberger, J. and Schuller, K.A. 1999. Glycolytic flux is adjusted to nitrogenase activity in nodules of detopped and argon-treated plants. *Plant Physiol.* 119: 445–453.
- Denison, R.F., Hunt, S. and Layzell, D.B. 1992. Nitrogenase activity, nodule respiration, and O₂ permeability following detopping of alfalfa and birdsfoot trefoil. *Plant Physiol.* 98: 894–900.
- Gordon, A.J. and Kessler, W. 1990. Defoliation induced stress in nodules of white clover. II. Immunological and enzymatic measurements of key proteins. *J. Exp. Bot.* 41: 1255–1262.
- Gordon, A.J., Kessler, W. and Minchin, F.R. 1990. Defoliation induced stress in nodules of white clover. I. Changes in physiological parameters and protein synthesis. *J. Exp. Bot.* 41: 1245–1253.
- Hammer, P.A., Tibbitts, T.W., Langhans, R.W. and McFarlane, J.C. 1978. Base-line growth studies of ‘Grand Rapids’ lettuce in controlled environments. *J. Am. Soc. Hort. Sci.* 103: 649–655.
- Hartwig, U.A. 1998. The regulation of symbiotic N₂ fixation: a conceptual model of N feedback from the ecosystem to the gene expression level. *Persp. Plant Ecol. Evol. Syst.* 1: 92–120.
- Hartwig, U., Boller, B. and N osberger, J. 1987. Oxygen supply limits nitrogenase activity of clover nodules after defoliation. *Ann. Bot.* 59: 285–291.
- Hartwig, U., Boller, B.C., Baur-H och, B. and N osberger, J. 1990. The influence of carbohydrate reserves on the response of nodulated white clover to defoliation. *Ann. Bot.* 65: 97–105.
- Hartwig, U.A., Heim, I., L uscher, A. and N osberger, J. 1994. The nitrogen-sink is involved in the regulation of nitrogenase activity in white clover after defoliation. *Physiol. Plant.* 92: 375–382.
- Heim, I., Hartwig, U.A. and N osberger, J. 1993. Current nitrogen fixation is involved in the regulation of nitrogenase activity in white clover (*Trifolium repens* L.). *Plant Physiol.* 103: 1009–1014.
- Herrin, D.L. and Schmidt, G.W. 1988. Rapid, reversible staining of Northern blots prior to hybridization. *BioTechniques* 6: 196.
- Johnson, R.R., Cranston, H.J., Chaverra, M.E. and Dyer, W.E. 1995. Characterization of cDNA clones for differentially expressed genes in embryos of dormant and nondormant *Avena fatua* L. caryopses. *Plant Mol. Biol.* 28: 113–122.
- Joshi, C.P. 1987. Putative polyadenylation signals in nuclear genes of higher plants: a compilation and analysis. *Nucl. Acids Res.* 15: 9627–9640.
- Lamb, C.J., Lawton, M.A., Dron, M. and Dixon, R.A. 1989. Signals and transduction mechanisms for activation of plant defenses against microbial attack. *Cell* 56: 215–224.
- Liang, P. and Pardee, A.B. 1992. Differential display of eukaryotic messenger RNA by means of the polymerase chain reaction. *Science* 257: 967–971.
- Liang, P., Averboukh, L. and Pardee, A.B. 1993. Distribution and cloning of eukaryotic mRNAs by means of differential display: refinements and optimization. *Nucl. Acids Res.* 21: 3269–3275.
- Liang, P., Zhu, W., Zhang, X., Guo, Z., O’Connell, R.P., Averboukh, L., Wang, F. and Pardee, A.B. 1994. Differential display using one-based anchored oligo-dT primers. *Nucl. Acids Res.* 22: 5763–5764.
- Minchin, F.R., Witty, J.F., Sheehy, J.E. and M uller, M. 1983. A major error in the acetylene reduction assay: decreases in nodular nitrogenase activity under assay conditions. *J. Exp. Bot.* 34: 641–649.
- Mohr, U., Lange, J., Boller, T., Wiemken, A. and V ogeli-Lange, R. 1998. Plant defense genes are induced in the compatible, but not in incompatible interaction between bean roots and *Fusarium solani*, and not during mycorrhizal root colonization by *Glomus mosseae*. *New Phytol.* 138: 589–598.
- Ryle, G.J.A., Powell, C.E. and Gordon, A.J. 1985. Short-term changes in CO₂ evolution associated with nitrogenase activity in white clover in response to defoliation and photosynthesis. *J. Exp. Bot.* 42: 637–638.
- Sambrook, J., Fritsch, E.F. and Maniatis, T. 1989. *Molecular Cloning: A Laboratory Manual*, 2nd ed., Cold Spring Harbor Laboratory Press, Plainview, NY.
- Sheehy, J.E., Minchin, F.R. and Witty, J.F. 1983. Biological control of the resistance to oxygen flux in nodules. *Ann. Bot.* 52: 565–571.
- V ogeli-Lange, R., B urckert, N., Boller, T. and Wiemken, A. 1996. Rapid selection and classification of positive clones generated by mRNA differential display. *Nucl. Acids Res.* 4: 1385–1386.
- V ogeli-Lange, R., B urckert, N., Boller, T. and Wiemken, A. 1997. Screening for positive clones generated by differential display. In: P. Liang and A.B. Pardee (Eds.) *Methods in Molecular Biology*, Vol. 85, Humana Press, Totowa, NJ, pp. 95–103.
- Weisbach, C., Hartwig, U.A., Heim, I. and N osberger, J. 1996. Whole-nodule carbon metabolites are not involved in the regulation of oxygen permeability and nitrogenase activity in white clover nodules. *Plant Physiol.* 110: 539–545.
- Witty, J.F., Minchin, F.R., Sheehy, J.E. and Ines Minguuez, M. 1984. Acetylene-induced changes in the oxygen diffusion resistance and nitrogenase activity of legume root nodules. *Ann. Bot.* 53: 13–20.
- Witty, J.F., Minchin, F.R., Sk ot, L. and Sheehy, J.E. 1986. Nitrogen fixation and oxygen limitation in legume root nodules. *Oxford Surv. Plant Mol. Cell Biol.* 3: 275–314.